GLOBAL CLIMATIC IMPACTS OF A COLLAPSE OF THE ATLANTIC THERMOHALINE CIRCULATION

MICHAEL VELLINGA and RICHARD A. WOOD

Met Office, Hadley Centre for Climate Prediction and Research, London Road, Bracknell RG12 2SY, United Kingdom

Abstract. Part of the uncertainty in predictions by climate models results from limited knowledge of the stability of the thermohaline circulation of the ocean. Here we provide estimates of the response of pre-industrial surface climate variables should the thermohaline circulation in the Atlantic Ocean collapse. For this we have used HadCM3, an ocean-atmosphere general circulation model that is run without flux adjustments. In this model a temporary collapse was forced by applying a strong initial freshening to the top layers of the North Atlantic. In the first five decades after the collapse surface air temperature response is dominated by cooling of much of the Northern Hemisphere (locally up to 8 °C, 1–2 °C on average) and weak warming of the Southern Hemisphere (locally up to 1 °C, 0.2 °C on average). Response is strongest around the North Atlantic but significant changes occur over the entire globe and highlight rapid teleconnections. Precipitation is reduced over large parts of the Northern Hemisphere. A southward shift of the Intertropical Convergence Zone over the Atlantic and eastern Pacific creates changes in precipitation that are particularly large in South America and Africa. Colder and drier conditions in much of the Northern Hemisphere reduce soil moisture and net primary productivity of the terrestrial vegetation. This is only partly compensated by more productivity in the Southern Hemisphere. The total global net primary productivity by the vegetation decreases by 5%. It should be noted, however, that in this version of the model the vegetation distribution cannot change, and atmospheric carbon levels are also fixed. After about 100 years the model's thermohaline circulation has largely recovered, and most climatic anomalies disappear.

1. Introduction

An important feature of present-day climate is that heat transport in the Atlantic Ocean is overall northward, rather than from the equator to the poles as in the Pacific Ocean (Ganachaud and Wunsch, 2000) and the atmosphere (Trenberth and Caron, 2001). This is a manifestation of the conveyor belt-like structure by which the thermohaline circulation of the ocean ('THC') organises the global heat transport (Gordon, 1986). The deep outflow of cold North Atlantic Deep Water is matched by a warm northward surface flow. This effectively transports heat into the North Atlantic which, when released, moderates climate in northwestern Europe.

Palaeoclimatic records suggest that this mode of ocean circulation is not unique. Different modes are believed to have occurred during glacial times and periods of deglaciation (Sarnthein et al., 1994). Numerical models too suggest that modern climate may have two possible stable states: one with and one without North Atlantic Deep Water ('NADW') formation, and associated presence or absence of

Climatic Change **54:** 251–267, 2002.

a vigorous THC (Manabe and Stouffer, 1999; Ganapolski et al., 2001). In these models the state without a vigorous THC has air temperatures in the Northern Hemisphere that locally can be up to 9 °C cooler. For some hybrid and intermediate complexity climate models it has been shown that equilibrium states of the THC form a hysteresis curve (cf. the brief overview by Rahmstorf, 2000). Large enough freshwater perturbations can trigger a transition from one equilibrium state to the other, while greenhouse gas concentrations are held fixed. Simulations have also shown a collapse of the THC under certain scenarios of increasing greenhouse gas concentrations (Manabe and Stouffer, 1994; Stocker and Schmittner, 1997; Rahmstorf and Ganapolski, 1999).

How likely it is that the THC might collapse in the near future is unclear, as there remains a large uncertainty in modelled stability of the present THC. (In this paper we use the term 'THC collapse' to denote a major disruption of the THC, not necessarily complete, nor permanent.) There is disagreement amongst general circulation models ('GCMs') about the response of the THC to increased greenhouse gas concentrations though none of these predict a complete THC collapse over the next century under an IS92a scenario (Cubasch et al., 2001). Additionally, particular climate feedbacks that are not always represented in some of the idealised models may cause the THC to have stability properties that are different from those in GCMs. In particular, changes to the ocean gyre transport and the hydrological cycle can act as important stabilising mechanisms for the THC (Latif et al., 2000; Thorpe et al., 2001; Vellinga et al., 2002). Questions about the likelihood of a collapse of the THC in this century are left aside here.

The question of what the climate response to an eventual collapse would be is an important one, both from physical and socio-economic points of view (Keller et al., 2000). Possible climate response to a THC collapse has been described before (Schiller et al., 1997; Manabe and Stouffer, 1988) using climate GCMs that require flux adjustments. These are artificial fluxes that prevent the models' control climate from drifting, but do so at the cost of obscuring the model response to a THC collapse (e.g., because they may modify the relationship between meridional heat transport and climate state).

The most recent version of the Met Office's Hadley Centre climate model (HadCM3) has maintained a stable climate simulation for over 1000 years without the use of flux adjustments (Gordon et al., 2000). It is a global atmosphere-ocean model with sea ice and land surface schemes. We have used this model to analyse the climate response caused by a forced collapse of the THC. In this paper we will describe the response in a number of quantities relating to surface climate conditions and where possible compare them to other estimates.

The present study is part of our ongoing efforts to reduce uncertainty in modelling of the THC stability in GCMs. We want to analyse the climate feedbacks after a disruption of the THC *per se*, i.e., in isolation from any anthropogenic climate forcing. We therefore have carried out the experiment in a pre-industrial climate state, with fixed concentrations of CO_2. The model response will also provide

an estimate for the uncertainty in climate predictions that is caused by any errors in predicting the THC stability. It will also give potential input to impacts models used to study the consequences of a THC collapse. Certain aspects of the transient climate response (such as the timing of events) may, however, be dependent on the design of this particular experiment.

A brief description of the model and the set-up of the experiment is given in Section 2. The climate response is given in Section 3. Conclusions follow in Section 4.

2. Model and Experimental Set-Up

The climate model that has been used in this study is HadCM3, a coupled ocean-atmosphere model, with sea-ice and land surface schemes. The atmosphere model has a resolution of $2.5° \times 3.75°$, with 19 vertical levels. The ocean model has a resolution of $1.25° \times 1.25°$ and has 20 vertical levels. The model maintains a stable surface climate (as measured by vanishing net radiative fluxes at the top of the atmosphere) throughout a control run of over 1000 years with fixed pre-industrial greenhouse gas concentrations, without the use of flux correction. Details of the model, a validation of its control climate and assessment of its errors are given by Gordon et al. (2000), Pope et al. (2000), Collins et al. (2001) and Pardaens et al. (2001). That experiment will be referred to as 'control run' throughout this paper. The model simulates a realistic ocean heat transport which is relevant to the results presented here. Wood et al. (1999) and Vellinga et al. (2002) present a validation of aspects of the THC.

We produced a weakened THC in the model by perturbing the state that the control integration of HadCM3 had reached after 100 years. The top 800 m of the North Atlantic ([80° W–20° E] × [50° N–90° N]) were made fresher by about 2 *psu*. Conservation of salt was assured by globally redistributing the salt taken out of the North Atlantic. The THC is sensitive to freshening of the upper layers of the ocean at high latitudes, as this inhibits the process of deep water formation (e.g. Bryan, 1986). Freshening of the North Atlantic has been used before as a means to disrupt the THC in GCMs (Manabe and Stouffer, 1995; Schiller et al., 1997). Our instantaneous salinity perturbation is equivalent to a freshwater pulse of about $6 \cdot 10^{14}$ m^3 (≈ 16 Sv $*$ year; 1 Sv $\equiv 10^6$ m^3 s^{-1}), assuming a reference salinity of 35 *psu*. It has the result that the THC collapses within 10 years (Figure 1). Schiller et al. (1997) apply an anomalous freshwater surface flux lasting for 500 years, amounting in total to more than 150 Sv $*$ year of fresh water; Manabe and Stouffer (1995) apply 10 Sv $*$ year.

After the instantaneous freshening was applied, the model was allowed to adjust freely to the new salinity field in an integration of 150 years, referred to as 'perturbation run'. We emphasize here that after about 120 years the THC had regained its original strength (Figure 1). Due to changes in precipitation in the

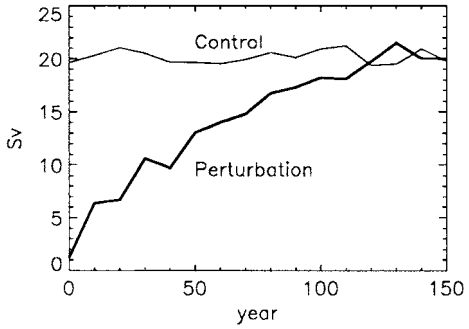

Figure 1. Timeseries of the strength of the THC in the perturbation run (heavy) and control run (light). Shown are decadal mean values of the meridional stream function in the Atlantic at 48° N, at 666 m depth.

tropical Atlantic and ocean freshwater transports, salinity in the high latitudes can recover, which leads to a re-establishment of the THC. Adjustment processes and climate feedbacks that drive this recovery are described by in detail by Vellinga et al. (2002). The responses in a number of surface climate variables are given in the next section.

3. Climate Response

Within 10 years after the salinity perturbation is applied the Atlantic THC (as measured by the zonally averaged meridional circulation) collapses (Figure 1). This eliminates the northward heat transport and associated heat release in the North Atlantic. As mentioned already the model is not in equilibrium during the first 100 years of the experiment. Even so, the transient climate response allows an assessment of the impact that a permanent THC collapse would have because of the rapid response in important ocean and atmosphere variables, such as ocean heat transport, sea surface temperature ('SST'), precipitation etc. The effects of the slowest components of the climate system (e.g., heat uptake by the deep ocean) on surface variables may, however, be underestimated in this transient climate state. To see to what extent anomalies spread globally we mostly present fields for years 20–30 of the experiment, even though the response around the North Atlantic is sometimes stronger in the first decade.

Climate response after the collapse of the THC is measured in terms of anomalies between the perturbation and the control experiments. To exclude any contribution to these anomalies that lie within the natural variability of the control climate, only anomalies that exceed two standard deviations (of the corresponding meaning period from the control experiment) are deemed significant.

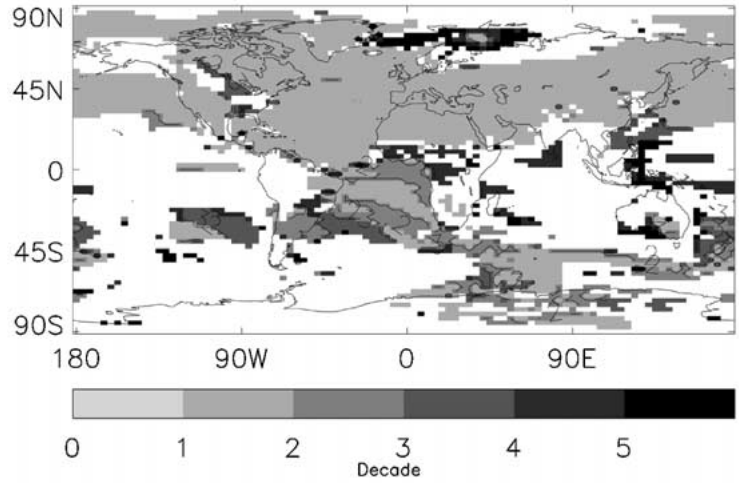

Figure 2. Spread of surface air temperature anomalies. The shading indicates the first decade in which a significant anomaly appears and persists for two or more decades.

The sequence of this analysis will be: surface air temperature (Section 3.1), surface winds (Section 3.2), precipitation and evaporation (Section 3.3) and implications for the vegetation (Section 3.4).

3.1. SURFACE AIR TEMPERATURE

The collapse of the THC causes rapid global change in surface air temperature (Figure 2). Within 20 years after the shutdown of the THC persistent anomalies (lasting two or more decades) have covered most of the Northern Hemisphere. In the Southern Hemisphere the response takes longer to become apparent, up to three decades.

The reduction of northward heat transport and surface heat release in the North Atlantic lead to significant cooling of the air in that area. Maximum cooling of up to 8 °C occurs over the northwest Atlantic. Over Europe the cooling is 1–3 °C in the third decade after the THC collapse (Figure 3).

The comparatively strong cooling over the northwest Atlantic and Labrador Sea and the Sea of Okhotsk is caused by increased sea-ice cover (Vellinga et al., 2002) that isolates the atmosphere from the relatively warm sea surface and augments the cooling. The atmospheric circulation effectively spreads the signal over large parts of the Northern Hemisphere. This results in significant cooling up to 2 °C over Asia and North America.

The Northern Hemisphere cooling occurs in both the boreal winter ('DJF') and summer ('JJA') months, but the effect is stronger in winter (Figure 5a). This inequality increases the amplitude of the seasonal cycle of the Northern Hemisphere by up to 1 °C. The areas with the strongest seasonal component in the temperature response are the Northwestern Atlantic and Labrador Sea and the Sea of Japan

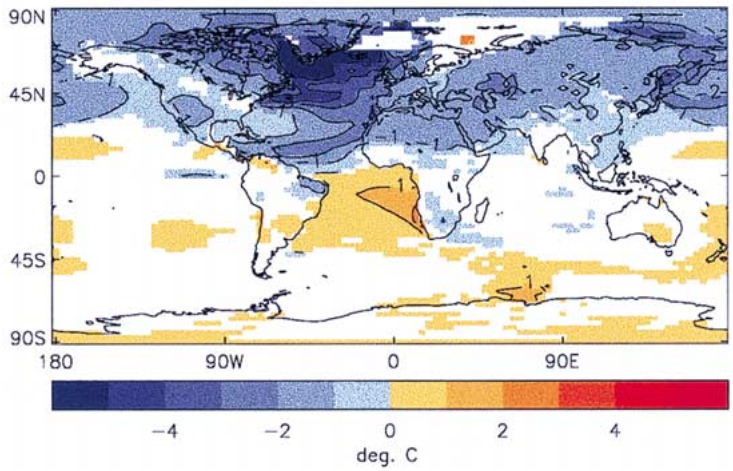

Figure 3. Change in surface air temperature during years 20–30 after the collapse of the THC. Areas where the anomaly is not significant have been masked.

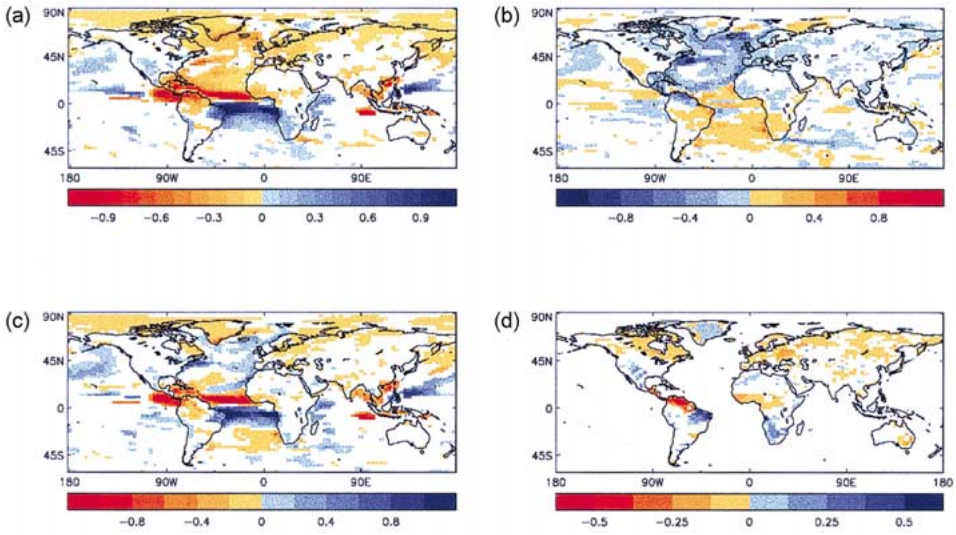

Figure 4. Significant changes during years 20–30 of the experiment of annual mean (a) precipitation (b) evaporation into the atmospheric boundary layer (c) precipitation surplus (d) net primary productivity. In (a)–(c) units are m year^{-1}, and blue (red) colours indicate anomalously wet (dry) conditions. Units in (d) are kg carbon m^{-2} year^{-1}.

and Sea of Okhotsk. Over the Labrador Sea DJF cooling of up to 16 °C occurs (not shown), compared to 8 °C for the annual mean. As mentioned before, these areas are covered by an anomalously large amount of sea ice. The sea ice cover is particularly extensive in DJF, a time of year when sea ice cover has a large control on surface air temperature. The anomalous sea ice cover melts during JJA, which allows for heat exchange between ocean and atmosphere, and abates the cooling.

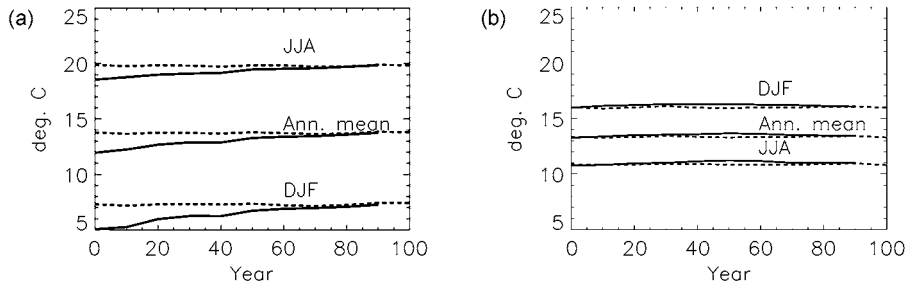

Figure 5. Average surface air temperature (in °C) in (a) the Northern Hemisphere (b) Southern Hemisphere. The solid lines show evolution of temperature in the perturbation run, the dashed lines show the same quantities for the unperturbed control climate. Shown are decadally averaged DJF, JJA and annual mean values.

The extremely cold DJF temperatures also affect the land areas adjacent to the seas affected by the sea ice cover (northern Canada and Greenland, eastern Siberia and northern Japan). Elsewhere, cooling in DJF is comparable to that of the annual mean cooling of Figure 3.

The Central England Temperature ('CET') dataset provides a continuous daily temperature record representative of central England for 1772–1991 (Parker et al., 1992), with monthly mean temperatures going back to 1659 (Manley, 1974). The length of this instrumental record makes it a valuable resource for analysing the frequency of extreme events (Jones et al., 1999). To put the simulated 3 °C cooling over Britain in years 20–30 after the THC collapse (Figure 3) into perspective it is worth pointing out that in the entire observed CET record prolonged cooling (two decades with annual mean cooling of around 1 °C relative to 1961–1990 averages or 'normals') occurs only once, at the end of the 17th century. The simulated cooling after a THC collapse is thus three times stronger than the cooling in Britain in the Little Ice Age (in the period for which there is an instrumental record).

In years 1–10 of the perturbation experiment the (model equivalent of) daily maximum CET is on average four degrees cooler than the normals of the control experiment. (Figure 6a). In a climate without THC the *average* maximum temperatures during spring and autumn in the model are colder than the coldest 5% of days that occur in the control experiment.

One has to treat the model CET data with some care because in the control run HadCM3 is colder than the observed values of 1961–1990 (Figure 6b), although the model's maximum CET data are well covered by 90% of the most commonly *observed* values between 1961–1990. The model (control) normals are colder than observed by 1.4 °C for the annual mean, and by 2 °C in DJF. There are various possible reasons for this, not necessarily mutually exclusive, and a full discussion is beyond the scope of this paper. It may be that systematic model errors create a cold bias. Additionally, due to natural variability the climates of this period of the control run and of the real world can be in different states (e.g., the phases

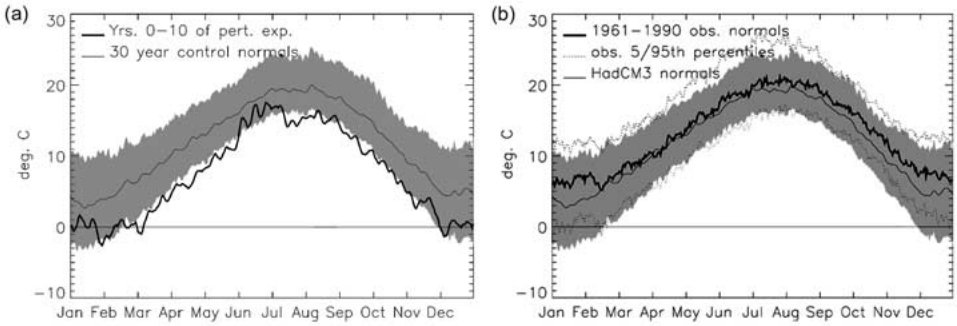

Figure 6. (a) Daily maximum temperature in central England in HadCM3. The thin curve shows normals for 30 years of the control run (taken from the period parallel to the perturbation experiment); its 5th and 95th percentile values are indicated by the shading. Smoothed values averaged over years 1–10 after THC collapse are shown by the heavy solid line. (b) Thin line and shading as in (a); the heavy solid line shows the observed maximum daily CET normals (Parker et al., 1992), the dotted line its 5th and 95th percentile values.

of the North Atlantic Oscillation (Hurrell, 1995) may be different at the time of sampling).

While the Northern Hemisphere cools the Southern Hemisphere warms, slightly; the average temperature rises by a few tenths of a degree (Figure 5b). Warming is strongest over the South Atlantic, up to 1 °C. Elsewhere there is a patchy pattern of warm anomalies emerging from the natural variability (Figure 2). It takes about 40 years before the maximum warming sets in, indicating slow adjustment of the oceans and atmospheric radiation budget. There is, however, a 'fast' route by which warm sea surface temperature anomalies leave the South Atlantic and rapidly propagate eastward on the Antarctic Circumpolar Current in the Southern Ocean. The Northern Hemisphere cooling and Southern Hemisphere warming persist for about 80 years.

The pattern and magnitude of Northern Hemisphere cooling of Figure 3 is comparable to that described by Manabe and Stouffer (1997), who forced a collapse of the THC in the GFDL climate model. The area of maximum cooling in their experiment is shifted to the east, but also shows widespread Northern Hemisphere cooling of about 1 °C. Schiller et al. (1997) quote values for maximum cooling of over 15 °C for the annual mean. Apparently the strong cooling in their model is caused by extensive growth of sea ice, partly created by the flux adjustment of heat. Weak Southern Hemisphere warming is a common response in the GCM experiments (Schiller et al., 1997; Manabe and Stouffer, 1997). In the CLIMBER-2 model Northern Hemisphere cooling associated with a climate state without THC (Ganapolski et al., 2001) has a pattern and amplitude similar to that in Figure 3. This model also simulates the enhanced DJF cooling of up to 15 °C over the North Atlantic found in HadCM3. The Southern Hemisphere warming in the CLIMBER-

2 model is a bit stronger than in the other models: it exceeds 2 °C over large parts of the Southern Ocean.

3.2. SURFACE PRESSURE AND WINDS

The temperature response in the atmosphere extends from the surface to the stratosphere, thereby changing the geopotential height field and general circulation of the atmosphere (see e.g. Peixoto and Oort (1992) for a basic introduction). We limit the discussion here to changes at a pressure of 1000 hPa. Exact positioning and other details of the anomaly pattern vary from decade to decade but the main features are robust during the first 100 years of the experiment. In the extratropics the response has a distinct seasonal component (Figure 7). In DJF the most important features are positive height anomalies over the subtropical North Atlantic and Europe, and negative height anomalies over the Greenland Sea and near the Aleutians. In DJF surface air temperature is particularly low over the Northwest Atlantic and Pacific Oceans, as discussed in Section 3.1. This creates a larger north-south temperature contrast across the atmospheric storm tracks over the North Atlantic and North Pacific Oceans. The storm tracks become more intense, and account for the anomalously low DJF pressure over those oceans (Figure 7a). In the extratropics the velocity response is more or less geostrophic, giving enhanced westerlies in the North Atlantic and the North Pacific of 1–2 m/s for the seasonal mean.

Over continental Europe the change in the pressure distribution results in a reduced penetration of maritime air. In the tropical Atlantic height anomalies drive an anomalous southward, cross-equatorial flow. This is related to an enhanced rising branch of the Hadley circulation during DJF and a southward shift of the ITCZ (Vellinga et al., 2002). This has large consequences for rainfall in Africa, Central America and northern South America (Section 3.3). The anomalous equatorial flow persists during JJA, but elsewhere in the Atlantic anomalies are weak. Significant changes are now prevalent in the Southern Ocean and the North Pacific.

To our knowledge there exist no relevant published results elsewhere to compare these changes to. Manabe and Stouffer (1988) report higher mean sea level pressure where cooling occurs in a climate without a THC (e.g., in the North Atlantic). The absence of a seasonal cycle in the solar radiation in their experiment makes a comparison difficult, as we have identified the prominence of seasonal variations in the response.

3.3. PRECIPITATION AND EVAPORATION

In contrast with the clear-cut north-south division of surface air temperature anomalies the response in precipitation exhibits a large spatial variation. The areas that experience the largest changes are the tropical Atlantic and the tropical Pacific (Figure 4a). This is a result from the southward shift of the ITCZ (Section 3.2). Precipitation anomalies associated with this shift are on the order of 0.8–1 m/year.

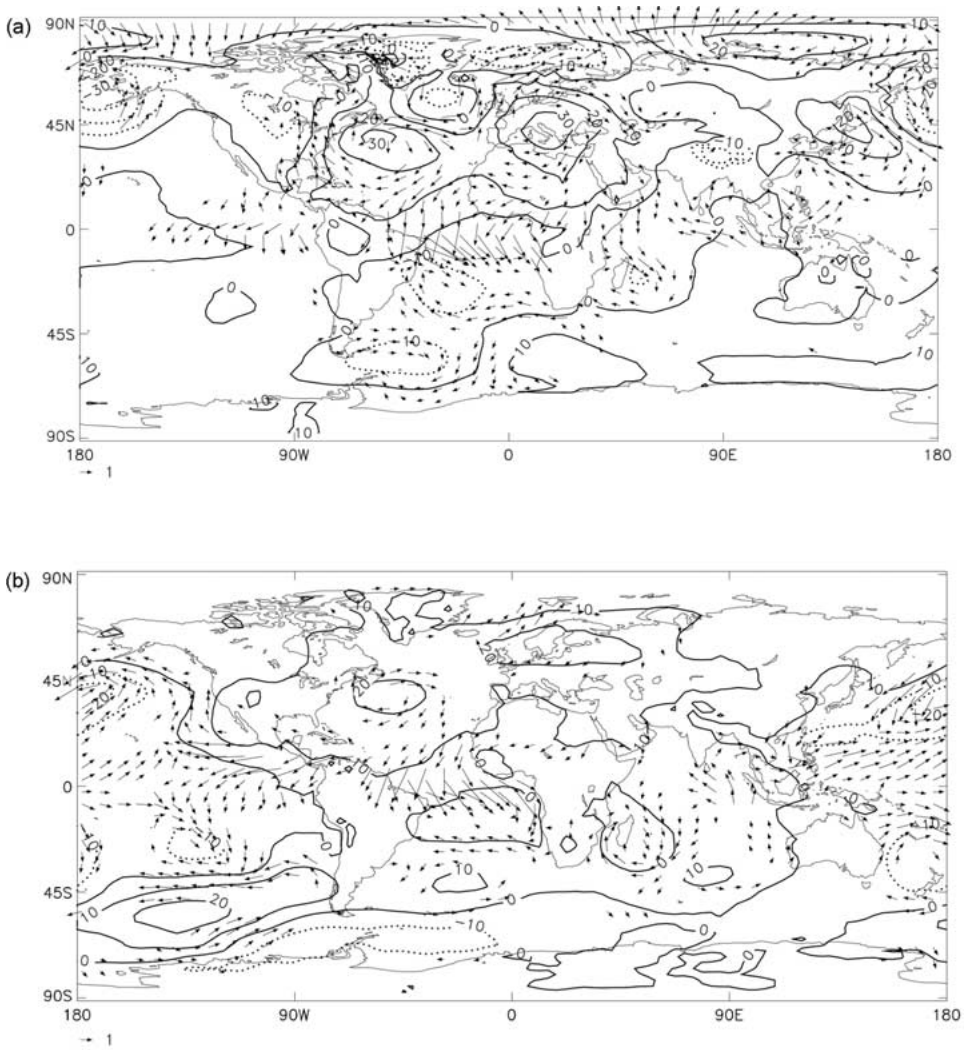

Figure 7. 1000 hPa height anomalies in m (contours) and significant velocity anomalies in m/s (arrows) for years 20–30 after the collapse of the THC. (a) Anomalies for DJF. (b) Anomalies for JJA.

A comparable response was reported by Schiller et al. (1997) and Manabe and Stouffer (1988). Rainfall in the Northern Hemisphere midlatitudes is reduced, consistent with the cooling: less water vapour can be held by colder air. Although the total amount of precipitation in Europe is reduced by about 0–0.2 m/year some of the high ground (Scotland, Norway, the Alps) receives significantly more snowfall (20–30 cm/year). Snow cover in northwest and central Europe lasts on average 1–2 months longer each year in the first decade after the THC collapse.

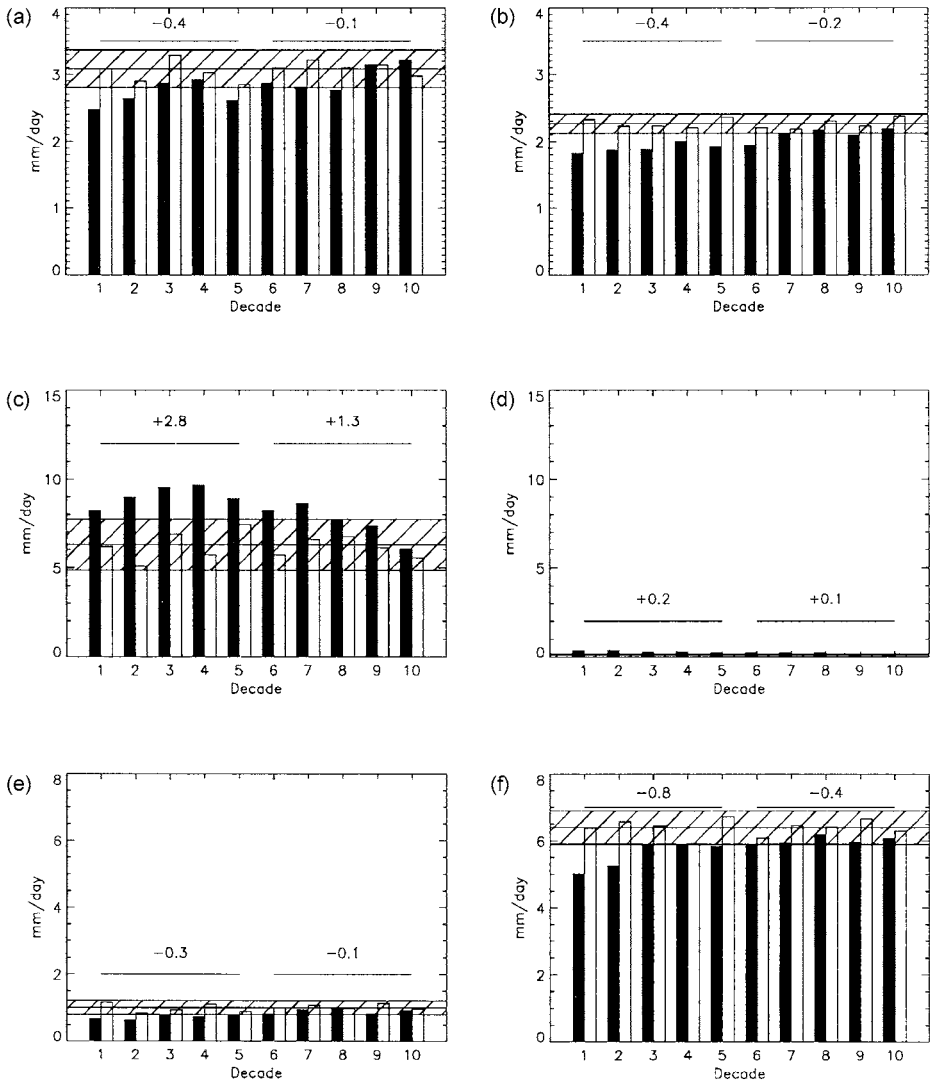

Figure 8. Average rainfall in mm/day for the perturbed climate (black bars) and the control climate (white bars). Average precipitation rate of the control run is shown by the central horizontal line, the hatching indicates the range occupied by ± 2 standard deviations. Average anomalies during the first and last 50 years of the perturbed climate are given by the numbers on top. (a) DJF western Europe; (b) JJA western Europe; (c) DJF north eastern Brasil; (d) JJA north eastern Brasil; (e) DJF Indian subcontinent; (f) JJA Indian subcontinent.

For a few areas Figure 8 illustrates the magnitude of precipitation anomalies, as well as their duration in summer and winter seasons. The reduction in precipitation in western Europe after the THC collapse is the same in both seasons (Figures 8a,b). In certain parts of the tropics the seasonal migration of the ITCZ creates a large seasonal cycle of rainfall. The changed positioning of the ITCZ due to the collapse of the THC introduces a seasonal component in the climate response; e.g., in eastern Brazil (Figures 8c,d) the wet season becomes significantly wetter, with little (absolute) change of rainfall in the dry season. During DJF the area of the tropical South Atlantic still receives more precipitation than under normal conditions. But unlike in JJA most of this falls over the ocean, and in DJF misses continental South America. Conversely, rainfall in Venezuela and central America is reduced by 1–1.5 mm/day in the first 50 years, a reduction of 30% in JJA and 50% in DJF. Over the Indian subcontinent (Figures 8e,f), DJF rainfall shows a decline that is typical for the Northern Hemisphere, caused by the cooling effect. But during JJA the southwest monsoon weakens (as measured by 850 hPa winds, not shown) which results in a stronger reduction of precipitation.

Evaporation changes (Figure 4b) reflect the north-south pattern of cooling-warming of surface air temperature and partly offsets the precipitation anomalies, notably over the North Atlantic Ocean. By and large the net effect (Figure 4c) is, however, dominated by precipitation.

3.4. VEGETATION NET PRIMARY PRODUCTIVITY

In addition to the ocean, atmosphere and sea-ice components HadCM3 also includes a land surface scheme (Cox et al., 1999). It defines geographically varying surface parameters, including contributions from 23 types of vegetation, that are averaged over each grid box. The fractional area of the vegetation types are geographically variable but constant in time. It is important to realise that in this experiment the distribution and type of vegetation cannot change in response to the altered external conditions, which it would do if an interactive vegetation scheme (Cox et al., 2000) were included.

Output from the land surface scheme includes soil moisture, and primary productivity and respiration of CO_2 by the terrestrial vegetation. These latter fields are purely diagnostic in HadCM3 since it does not include a carbon cycle. The difference between gross primary productivity and respiration is net primary productivity, a measure of the yield or harvest of the vegetation. It depends on factors such as soil moisture content, air temperature and incoming shortwave radiation. In a coupled climate-carbon cycle model (Cox et al., 2000) a steady state would be achieved when carbon fluxes due to mortality and net primary productivity balance.

The response in net primary productivity of the vegetation (Figure 4d) to the climate perturbation reflects the changed atmospheric conditions, and follows the pattern of precipitation surplus (Figure 4c). It has a strong similarity to the pattern of soil moisture anomalies (not shown). The colder and drier conditions over Eura-

Table I

Net primary productivity by the vegetation, integrated over the respective continental landmasses, in Gton carbon per year. Shown are the mean values and standard deviations for the control experiment (first two columns), the mean for the first 30 years of the perturbation experiment (third column), and the anomaly during the first 30 years, with significant anomalies in bold (fourth column). The negative primary productivity in Central America means the vegetation cannot be sustained and would die back in a fully interactive vegetation scheme

	Control mean	Standard deviation	Perturbation mean	Anomaly
Australia	3.5	0.2	3.2	–0.3
Asia	12.3	0.1	11.2	**–1.2**
Indian Subcontinent	0.90	0.07	0.57	**–0.32**
Europe	5.5	0.1	4.6	**–0.9**
Africa	8.4	0.3	8.4	0
North America	8.4	0.2	8.6	+0.1
Central America	0.34	0.08	–0.03	**–0.37**
South America	11.5	0.3	11.4	–0.1
NH	35.1	0.4	31.3	**–3.8**
SH	17.2	0.5	18.2	**+1.1**
Globe	52.2	0.7	49.5	**–2.8**

sia cause reductions in net primary productivity of order $\mathcal{O}(10\%)$ here (Table I). Central-America is particularly strongly affected, due to the lower rainfall. Here net primary productivity becomes negative (Table I, third column) and in a dynamic scheme vegetation would start to die back. In Africa, North and South America the large regional differences cancel out in the totals (cf. shift of ITCZ and the rainfall over South America; wetter conditions in southern North America, colder and drier in the north). The global integral shows a reduction of about 3 Gton C/year. In a climate model with active vegetation and carbon components, a fraction of the vegetation would have died as a result and some of the associated carbon would have been released to the atmosphere as CO_2, introducing a feedback between THC and carbon cycle. However, in this version of the model, the actual atmospheric CO_2 level is constant.

The oceanic carbon cycle is sensitive to changes in SST (which affects carbon solubility), to the amount of sea ice cover, and to the amount of vertical mixing and deep water formation that ventilates the deep ocean, (e.g. Sarmiento et al., 1998). To determine how significant the changes in the terrestrial carbon cycle from Table I are, compared to those that a THC collapse would cause to the oceanic carbon cycle, requires a study with a coupled climate carbon-cycle model (Cox et al., 2000).

4. Conclusions

We analysed the climate response in HadCM3, a state of the art climate model without flux adjustments, after the Atlantic thermohaline circulation ('THC') was suppressed by a large, instantaneous input of freshwater into the North Atlantic. Greenhouse gas concentrations were held fixed at pre-industrial levels in this experiment.⋆ Other experiments with HadCM3 do not predict a collapse of the THC in the next century under various climate forcing scenarios (Wood et al., 1999; Thorpe et al., 2001). But processes controling the stability of the THC – in models and in the real world – are currently not completely understood, and the response that we have described provides an estimate on the uncertainty in climate predictions that could be caused by incorrectly modelling the stability of the THC. Furthermore, the climate response could be used in studies of the impacts that a THC collapse would have. No attempt has been made here to estimate the likelihood of such an event.

Temperature response is strongest around the North Atlantic, but covers large parts of the globe within two decades. In the first 50 years strong cooling in the Northern Hemisphere (1–2 °C) is only partly offset by weak warming in the Southern Hemisphere (0–0.5 °C). Regional cooling over Europe and eastern North America is 1–2 °C in years 20–30, with maximum cooling of 8 °C over the northwest Atlantic.

Significant changes in the global distributions of surface winds, rainfall, evaporation and soil moisture stress the active role that the THC plays in shaping global climate. Results also suggest that a THC collapse could lead to a global reduction in net primary production by the terrestrial vegetation of about 5%. The model used here does not include carbon cycle feedbacks and one must treat this particular result with caution.

The predicted global warming over the next century due to rising greenhouse gas and aerosol concentrations is estimated to lie between 1.4–5.8 °C (Cubasch et al., 2001). The global temperature change due to a collapse of the Atlantic THC in a pre-industrial climate varies from –1 °C in the first decade to about –0.3 °C in years 40–50 (Vellinga et al., 2002). Local temperature change immediately after a THC collapse is much stronger than this. If, without any *a priori* justification, we assume a simple linear superposition, the cooling due to a hypothetical THC collapse would outweigh the warming around the North Atlantic that occurs in this model under an SRES B2 scenario (Johns et al., 2001), during the 21st century.

This study highlights the need to reduce the uncertainties in our climate models regarding the stability of the THC. A major disruption to the THC can have significant impacts on global and especially regional climate simulations. Even though the current generation of climate GCMs do not suggest that a collapse of the THC over the next 100 years is imminent (Cubasch et al., 2001), the potential for a

⋆ Additional data from this experiment can be made available on request.

large and rapid climate response in the case of such an event makes THC stability an important factor in assessing climate change (Rahmstorf, 1999; Mastrandrea and Schneider, 2001). To increase our confidence in simulations of future climate we need to reduce the uncertainty in modelling the stability of the THC. Efforts to reduce the uncertainty in HadCM3 are ongoing. This has started with the analysis of the dominant physical processes that determine size and nature of the response by the THC when it is subjected to various kinds of stress (Thorpe et al., 2001; Vellinga et al., 2002). In the next stage one would then attempt to eliminate modelling errors from these same processes.

Acknowledgements

We like to thank Peter Cox, Steven Spall, Jonathan Gregory, Howard Cattle and Geoff Jenkins for suggestions and stimulating discussions; Briony Horton for making the CET data available, and Ian Macadam for calculating the model CET data. Comments by Mike Hulme, Klaus Keller, Stefan Rahmstorf and two anonymous reviewers have helped to clarify the manuscript, and are thankfully acknowledged. This work was funded by the Department of the Environment, Food and Rural Affairs under the Climate Prediction Programme PECD/7/12/37.

References

Bryan, F.: 1986, 'High-Latitude Salinity Effects and Interhemispheric Thermohaline Circulations', *Nature* **323**, 301–304.

Collins, M., Tett, S. F. B., and Cooper, C.: 2001, 'The Internal Climate Variability of HadCM3, a Version of the Hadley Centre Coupled Model without Flux Adjustments', *Clim. Dyn.* **17**, 61–81.

Cox, P. M., Betts, R. A., Bunton, C. B., Essery, R. L. H., Rowntree, P. R., and Smith, J.: 1999, 'The Impact of New Land Surface Physics on the GCM Simulation of Climate and Climate Sensitivity', *Clim. Dyn.* **15**, 183–203.

Cox, P. M., Betts, R. A., Jones, C. D., Spall, S. A., and Totterdell, I. J.: 2000, 'Acceleration of Global Warming Due to Carbon-Cycle Feedbacks in a Coupled Climate Model', *Nature* **408**, 184–187.

Cubasch, U., Meehl, G. A., Boer. G. J., Stouffer, R. J., Dix, M., Noda, A., Senior, C. A., Raper, S. C. B., and Yap, K. S.: 2001, 'Projections of Future Climate Change', in Houghton, J. T., Ding, Y., Griggs, D. J., Noguer, M., van der Linden, P., Dai, X., Maskell, K., and Johnson, C. I. (eds.), *Climate Change 2001: The Scientific Basis. Contribution of Working Group I to the Third Assessment Report of the Intergovernmental Panel on Climate Change*, Cambridge University Press, pp. 525–582.

Ganachaud, A. and Wunsch, C.: 2000, 'Improved Estimates of Global Ocean Circulation, Heat Transport and Mixing from Hydrographic Data', *Nature* **408**, 453–457.

Ganapolski, A., Petoukhov, V., Rahmstorf, S., Brovkin, V., Claussen, M., Eliseev, A., and Kubatzki, C.: 2001, 'CLIMBER-2: A Climate System Model of Intermediate Complexity. Part II: Model Sensitivity', *Clim. Dyn.* **17**, 735–751.

Gordon, A. L.: 1986, 'Inter-Ocean Exchange of Thermocline Water', *J. Geophys. Res.* **91**, 5037–5046.

Gordon, C., Cooper, C., Senior, C. A., Banks, H., Gregory, J. M., Johns, T. C., Mitchell, J. F. B., and Wood, R. A.: 2000, 'The Simulation of SST, Sea Ice Extents and Ocean Heat Transports in a Version of the Hadley Centre Coupled Model without Flux Adjustments', *Clim. Dyn.* **16**, 147–168.

Hurrell, J.: 1995, 'Decadal Trends in the North Atlantic Oscillation: Regional Temperatures and Precipitation', *Science* **269**, 676–679.

Johns, T. C., Gregory, J. M., Ingram, W. J., Johnson, C. E., Jones, A., Lowe, J. A., Mitchell, J. F. B., Roberts, D. L., Sexton, D. M. H., Stevenson, D. S., Tett, S. F. B., and Woodage, M. J.: 2001, *Anthropogenic Climate Change for 1860 to 2100 Simulated with the HadCM3 Model under Updated Emissions Scenarios*, Hadley Centre Technical Note 22, Hadley Centre, (URL http://www.metoffice.com/research/hadleycentre/pubs/HCTN/HCTN_22.pdf).

Jones, P., Horton, E., Folland, C., Hulme, M., Parker, D., and Basnett, T.: 1999, 'The Use of Indices to Identify Changes in Climatic Extremes', *Clim. Change* **42**, 131–149.

Keller, K., Tan, K., Morel, F., and Braidford, D.: 2000, 'Preserving the Ocean Circulation: Implications for Climate Policy', *Clim. Change* **47**, 17–43.

Latif, M., Roeckner, E., Mikolajewicz, U., and Voss, R.: 2000, 'Tropical Stabilisation of the Thermohaline Circulation in a Greenhouse Warming Simulation', *J. Climate* **13**, 1809–1813.

Manabe, S. and Stouffer, R. J.: 1988, 'Two Stable Equilibria of a Coupled Ocean-Atmosphere Model', *J. Climate* **1**, 841–866.

Manabe, S. and Stouffer, R. J.: 1994, 'Multiple Century Response of a Coupled Ocean-Atmosphere Model to an Increase of Atmospheric Carbon Dioxide', *J. Climate* **7**, 5–23.

Manabe, S. and Stouffer, R. J.: 1995, 'Simulation of Abrupt Climatic Change Induced by Freshwater Input to the North Atlantic Oocean', *Nature* **378**, 165–167.

Manabe, S. and Stouffer, R. J.: 1997, 'Coupled Ocean-Atmosphere Model Response to Freshwater Input: Comparison with Younger Dryas Event', *Paleoceanography* **12**, 321–336.

Manabe, S. and Stouffer, R. J.: 1999, 'Are Two Modes of Thermohaline Circulation Stable?', *Tellus* **51A**, 400–411.

Manley, G.: 1974, 'Central England Temperatures, Monthly Means 1659 to 1973', *Quart. J. Roy. Meteorol. Soc.* **79**, 242–261.

Mastrandrea, M. and Schneider, S.: 2001, 'Integrated Assessment of Abrupt Climatic Changes', *Climate Policy* **1**, 433–449.

Pardaens, A., Banks, H., Gregory, J., and Rowntree, P.: 2001, 'Freshwater Transports in HadCM3', *Clim. Dyn.*, submitted.

Parker, D. E., Legg, T. P., and Folland, C. K.: 1992, 'A New Daily Central England Temperature Series', *Int. J. Clim.* **12**, 317–342.

Peixoto, J. P. and Oort, A. H.: 1992, *Physics of Climate*, American Institute of Physics, New York.

Pope, V. D., Gallani, M. L., Rowntree, P. R., and Stratton, R. A.: 2000, 'The Impact of New Physical Parametrizations in the Hadley Centre Climate Model – HadAM3', *Clim. Dyn.* **16**, 123–146.

Rahmstorf, S.: 1999, 'Shifting Seas in the Greenhouse?', *Nature* **399**, 523–524.

Rahmstorf, S.: 2000, 'The Thermohaline Ocean Circulation: A System with Dangerous Thresholds?', *Clim. Change* **46**, 247–256.

Rahmstorf, S. and Ganapolski, A.: 1999, 'Long-Term Global Warming Scenarios Computed with an Efficient Coupled Climate Model', *Clim. Change* **43**, 353–367.

Sarmiento, J., Hughes, T., Stouffer, R., and Manabe, S.: 1998, 'Simulated Response of the Ocean Carbon Cycle to Anthropogenic Climate Warming', *Nature* **393**, 245–249.

Sarnthein, M., Winn, K., Jung, S. J. A., Duplessy, J. C., and Labeyrie, L. et al.: 1994, 'Changes in East Atlantic Deep Water Circulation over the Last 30,000 Years: Eight Time Slice Reconstructions', *Paleoceanography* **9**, 209–267.

Schiller, A., Mikolajewicz, U., and Voss, R.: 1997, 'The Stability of the Thermohaline Circulation in a Coupled Ocean-Atmosphere General Circulation Model', *Clim. Dyn.* **13**, 325–347.

Stocker, T. and Schmittner, A.: 1997, 'Influence of CO_2 Emission Rates on the Stability of the Thermohaline Circulation', *Nature* **388**, 862–865.

Thorpe, R. B., Gregory, J. M., Johns, T. C., Wood, R. A., and Mitchell, J. F. B.: 2001, 'Mechanisms Determining the Atlantic Thermohaline Circulation Response to Greenhouse Gas Forcing in a Non-Flux-Adjusted Coupled Climate Model', *J. Climate* **14**, 3102–3116.

Trenberth, K. E. and Caron, J. M.: 2001, 'Estimates of Meridional Atmosphere and Ocean Heat Transports', *J. Climate* **14**, 3433–3443.

Vellinga, M., Wood, R. A., and Gregory, J. M.: 2002, 'Processes Governing the Recovery of a Perturbed Thermohaline Circulation in HadCM3', *J. Climate* **15**, 764–780.

Wood, R. A., Keen, A. B., Mitchell, J. F. B., and Gregory, J. M.: 1999, 'Changing Spatial Structure of the Thermohaline Circulation in Response to Atmospheric CO_2 Forcing in a Climate Model', *Nature* **399**, 572–575.

(Received 28 February 2001; in revised form 18 December 2001)